ACS Chemical Neuroscience

Research Article

pubs.acs.org/chemneuro

Binding Mode of an α-Amino Acid-Linked Quinoxaline-2,3-dione Analogue at Glutamate Receptor Subtype GluK1

Charles S. Demmer,[†] Charlotte Møller,[‡] Patricia M. G. E. Brown,[#] Liwei Han,[∥] Darryl S. Pickering,[∥] Birgitte Nielsen,[§] Derek Bowie,[#] Karla Frydenvang,[‡] Jette S. Kastrup,*[,‡] and Lennart Bunch*[,†]

[†]Chemical Neuroscience Group, [‡]Biostructural Research Group, [§]Medicinal Chemistry Group, [∥]Molecular and Cellular Pharmacology Group, and [⊥]Molecular Pharmacology Group, Department of Drug Design and Pharmacology, Faculty of Health and Medical Sciences, University of Copenhagen, Copenhagen, Denmark

[#]Bowie Lab, Department of Pharmacology & Therapeutics, Faculty of Medicine, McGill University, Montreal, Canada H3G 0B1

Supporting Information

ABSTRACT: Two α-amino acid-functionalized quinoxalines, **1a** (CNG-10301) and **1b** (CNG-10300), of a quinoxaline moiety coupled to an amino acid moiety were designed, synthesized, and characterized pharmacologically. While **1a** displayed low affinity at native AMPA, KA, and NMDA receptors, and at homomeric GluK1,3 receptors, the affinity for GluK2 was in the midmicromolar range (K_i = 136 μM), **1b** displayed low to midmicromolar range binding affinity at all the iGluRs (K_i = 9−126 μM). In functional experiments (outside-out patches excised from transfected HEK293T cells), 100 μM **1a** partially blocked GluK1 (33% peak response), while GluK2 was unaffected (96% peak response). Furthermore, **1a** was shown not to be an agonist at GluK1 and GluK2 at 100 μM. On the other hand, 100 μM **1b** fully antagonized GluK1 (8% peak response) but only partially blocked GluK2 (33% peak response). An X-ray structure at 2.3 Å resolution of **1b** in the GluK1-LBD (ligand-binding domain) disclosed an unexpected binding mode compared to the predictions made during the design phase; the quinoxaline moiety remains to act as an amino acid bioisostere, but the amino acid moiety is oriented into a new area within the GluK1 receptor. The structure of the GluK1-LBD with **1b** showed a large variation in domain openings of the three molecules from 25° to 49°, demonstrating that the GluK1-LBD is capable of undergoing major domain movements.

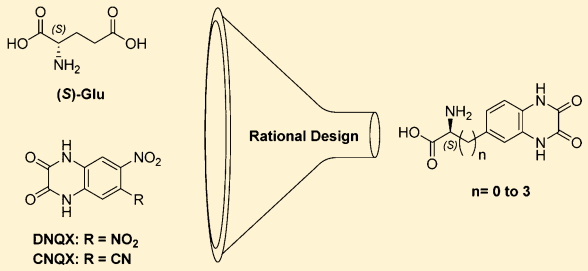

KEYWORDS: *Design, synthesis, radioligand binding, X-ray crystallography, domain opening*

INTRODUCTION

The common α-amino acid (*S*)-glutamate (Glu) is the major excitatory neurotransmitter of the mammalian central nervous system (CNS). The glutamatergic neurotransmitter system is involved in a vast number of neurological processes such as memory and learning, plasticity, and motor function,[1,2] and thus also in the pathogenesis of many neurological and psychiatric disorders. The class of fast-acting ionotropic Glu receptors (iGluRs) is divided into three groups that again comprise a number of subunits [AMPA receptors GluA1−4, kainic acid (KA) receptors[3−5] GluK1−5, and NMDA receptors[6] GluN1, GluN2A-D, and GluN3A,B]. The iGluRs form ligand-gated ion channels consisting of four subunits, with each subunit having an extracellular region composed of the N-terminal domain and the ligand-binding domain (LBD), a transmembrane region, and a C-terminal region. The LBD forms a clamshell-like domain with the glutamate-binding site located within two lobes designated D1 and D2.

A number of competitive antagonists that discriminate among the AMPA, KA, and NMDA receptors have been reported.[7] However, it remains a challenge to discover antagonists, which display selectivity among the subunits within one of these groups. In fact, only GluK1-selective competitive antagonists have been reported to date [e.g., LY466195[8] (Figure 1 and Table 1].[7] There is therefore an unmet need for the creative design of new chemical scaffolds that eventually can be developed into antagonists with a novel subunit selectivity profile. Such chemical probes are key tools in the elucidation of the role and function of Glu receptors in health and disease.

RESULTS AND DISCUSSION

Design. Some 20 years ago, a series of substituted quinoxaline-2,3(1*H*,4*H*)-diones [DNQX and CNQX (Figure 1 and Table 1)] were identified as potent competitive AMPA/KA receptor antagonists.[9] Interestingly, the quinoxaline-2,3-(1*H*,4*H*)-dione moiety acts as an α-amino acid bioisostere[10] as disclosed by X-ray crystallographic studies.[11,12]

A potentially new class of iGluR antagonists was designed with the general molecular formula I (Figure 2). Via the linkage of an α-amino acid to the quinoxaline-2,3(1*H*,4*H*)-dione

Received: September 23, 2014
Accepted: March 26, 2015

DOI: 10.1021/acschemneuro.5b00038
ACS Chem. Neurosci. XXXX, XXX, XXX−XXX

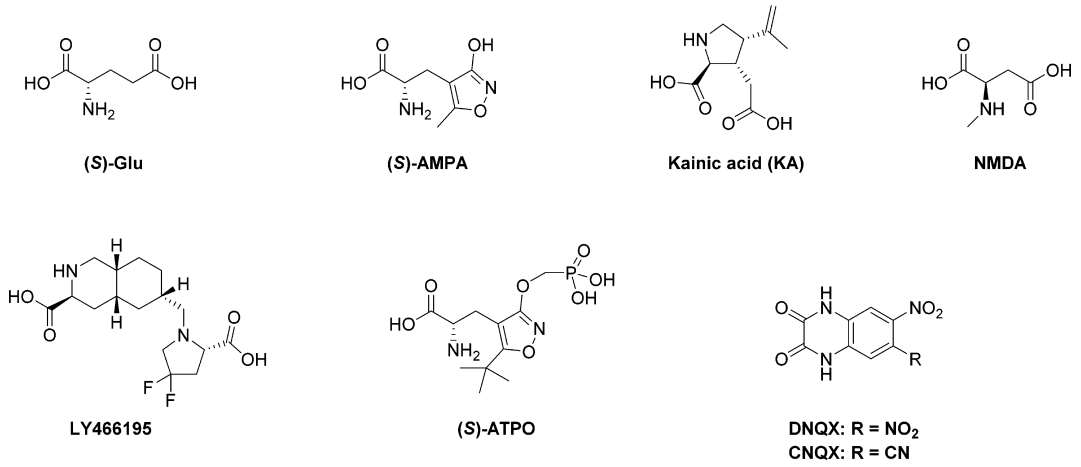

Figure 1. Chemical structures of Glu, AMPA, KA, NMDA, and competitive antagonists LY466195, (*S*)-ATPO, DNQX, and CNQX.

Table 1. Pharmacological Profiles of LY466195, ATPO, DNQX, CNQX, 1a (CNG-10301), and 1b (CNG-10300) at the iGluRs, Together with Binding Affinities of 1b at the GluK1-LBD[a]

	AMPA IC_{50}[b]	KA IC_{50}[b]	NMDA K_i[b]	GluA2 K_i[c]	GluK1 K_i[c]	GluK2 K_i[c]	GluK3 K_i[c]	GluK1-LBD K_i[c]
LY466195[d]	–	–	–	270	0.05	–	8.9	–
ATPO	16	>100	>100	60.3 ± 4.7	2.55 ± 0.43	>100	>1,000	–
DNQX	0.25[e]	0.53[e]	4.1[e]	0.254 ± 0.014	0.652 ± 0.028	2.10 ± 0.32	0.362 ± 0.033	–
CNQX	0.40[e]	0.27[e]	13[e]	0.333 ± 0.028	1.28 ± 0.30	1.49 ± 0.01	0.637 ± 0.050	–
1a (CNG-10301)	203 [3.69 ± 0.03]	>300	>200	>100 (80 ± 8%)	>100 (74 ± 3%)	136 ± 22	>100 (71 ± 5%)	–
1b (CNG-10300)	26 [4.59 ± 0.06]	126 [3.90 ± 0.02]	78 [4.12 ± 0.08]	21.3 ± 2.4	16.1 ± 1.0	9.52 ± 1.15	59.0 ± 3.2	37.1 ± 7.8

[a]All values are in micromolar. [b]Mean values ± the standard error of the mean (SEM) of three individual experiments. The following radioligands were used: AMPA receptors, [^{3}H]AMPA; KA receptors, [^{3}H]KA; NMDA receptors, [^{3}H]CGP 39653. [c]Mean values ± SEM of at least three experiments, conducted in triplicate at 12−16 ligand concentrations. In parentheses are values of percent residual specific binding at 100 μM ligand. The following radioligands were used: GluA2, [^{3}H]AMPA; GluK1−3, [^{3}H]-(2*S*,4*R*)-4-methyl-Glu (SYM2081) or [^{3}H]KA. Hill coefficients were not different from unity. [d]From ref 8. [e]Functional data from ref 9.

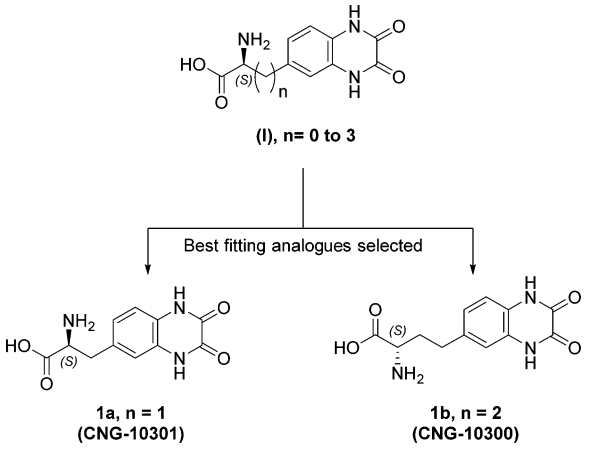

Figure 2. Design of α-amino acid-functionalized quinoxalines **1a** (CNG-10301) and **1b** (CNG-10300) as potential AMPA/KA antagonists.

moiety, the latter was initially assumed to act as a carboxylic acid bioisostere engaging in hydrogen bonding directly to the amino acid residues of the D2 domain of the receptor, or via water molecules. The pK_a value of an unsubstituted quinoxaline-2,3(1*H*,4*H*)-dione skeleton has been determined to be 9.2,[13] which calculates to approximately 1% of the ionized form at physiological pH 7.4.[10] The suitable linker length was investigated by performing a stochastic conformational search of chemical structures of the general formula I, for n = 0−3 (Figure 2). While a large variety of AMPA/KA receptor antagonists have been crystallized with GluA2-LBD and/or GluK1-LBD, the two distinct antagonists, ATPO [K_i = 2.6 μM affinity for GluK1, Protein Data Bank (PDB) entry 1VSO][14] and LY466195 (K_i = 0.05 μM affinity for GluK1,[8] PDB entry 2QS4),[15] were used as templates in the design. The study led to the conclusion that the linker length of n = 1, compound **1a** (Figure 3A) and the linker length of n = 2, compound **1b** (Figure 3B) were both attractive. In detail, one low-energy conformation of **1a** fit the pharmacophore dictated by LY466195, whereas four low-energy conformations of **1b** could be superimposed on LY466195, two being the most favorable. In comparison with LY466195, **1a** and **1b** present their hydrogen bonding functionalities to the receptor with altered distances and angles (Figure 3A,B). Such properties are in particular interesting as we were aiming to discover new scaffolds with unprecedented receptor subtype selectivity profiles.

Synthesis. A retrosynthetic analysis of target compounds **1a** and **1b** suggested the use of a protected natural α-amino acid (commercially available) as a direct source of chirality, and a Negishi cross coupling between the 6-quinoxaline moiety and the side chain of the amino acid was planned as the key step.[16,17] The synthesis of **1a** and **1b** commenced with the reduction of the carboxylic acid functionality of BOC-Asp-OBn

DOI: 10.1021/acschemneuro.5b00038
ACS Chem. Neurosci. XXXX, XXX, XXX−XXX

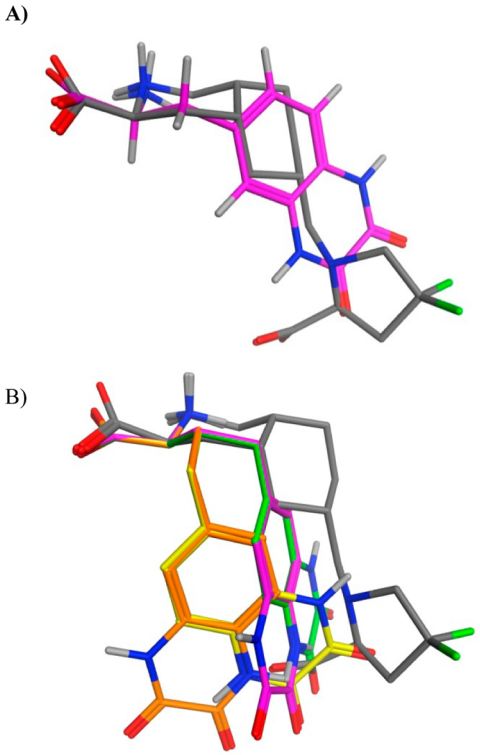

Figure 3. (A) Superimposition of a low-energy conformation of **1a** (purple) on LY466195 (gray; PDB entry 2QS4). Both compounds are colored according to atom type. (B) Superimposition of four low-energy conformations of **1b** ($\Delta\Delta G$ = 0−1 kcal/mol; yellow, orange, purple, and green) on LY466195.

2 to give the corresponding alcohol **3b**, using isobutyl chloroformate as an activator.[18] The crude product was used without further purification as this led to formation of the corresponding cyclization product due to the acidic nature of silica gel. The iodo-amino acids, **4a** and **4b**, were then generated from their corresponding alcohols **3a** (commercially available) and **3b**, respectively, by reaction with iodine under neutral conditions (triphenylphosphine and imidazole).[19] The quinoxaline moiety was successfully introduced by a palladium coupling with the organic zinc nucleophile (Negishi) from **4a** or **4b** and 6-bromo-2,3-dimethoxyquinoxaline **9**.[17] The palladium-catalyzed cross coupling was first tried out on **7** but proved to be unsuccessful, presumably because of the competing coordination of the 2,3-dicarbonyl oxygens. Possibly expectedly, 2,3-dichloroquinoxaline **8** was also unsuccessful as a coupling partner, giving a complex product mixture. Finally, **5a** and **5b** were fully deprotected in a one-pot reaction under acidic conditions, providing the HCl salt of the two target structures **1a** and **1b** (Scheme 1).

Pharmacology. With the two target compounds **1a** and **1b** in hand, they were characterized pharmacologically at rat synaptosomes (native AMPA, KA, and NMDA receptors). The compounds were also assessed at cloned homomeric GluA2 and GluK1−3 receptors, and all results are summarized in Table 1. Analogue **1a** displayed a low affinity for native iGluRs (IC_{50} or K_i of >200 μM) and cloned homomeric GluA2 and GluK1,3 receptors (K_i > 100 μM), and medium-range micromolar affinity for GluK2 (K_i = 136 μM). Analogue **1b** displayed medium-range micromolar affinity for native AMPA, KA, and NMDA receptors. The binding affinity of **1b** for AMPA receptors was confirmed at the cloned homomeric GluA2 receptor (K_i = 21 μM). At cloned homomeric GluK1−3 receptors, **1b** displayed medium-range binding affinity for GluK1−3 with K_i values of 16, 9.5, and 59 μM, respectively (Table 1). Finally, in a functional EAAT assay,[20] both **1a** and **1b** displayed no appreciable activity as inhibitors at subtypes EAAT1−3 [IC_{50} > 1000 μM (results not shown)].

Upon comparison with the four antagonists employed in the design phase [LY466195, ATPO, CNQX, and DNQX (Figure 1 and Table 1)], the broad profile of **1b** is comparable to that of DNQX and CNQX. On the other hand, a slightly GluK2 preferring profile of **1a** is surprising because LY466195 is highly

Scheme 1. Synthesis of 1a and 1b[a]

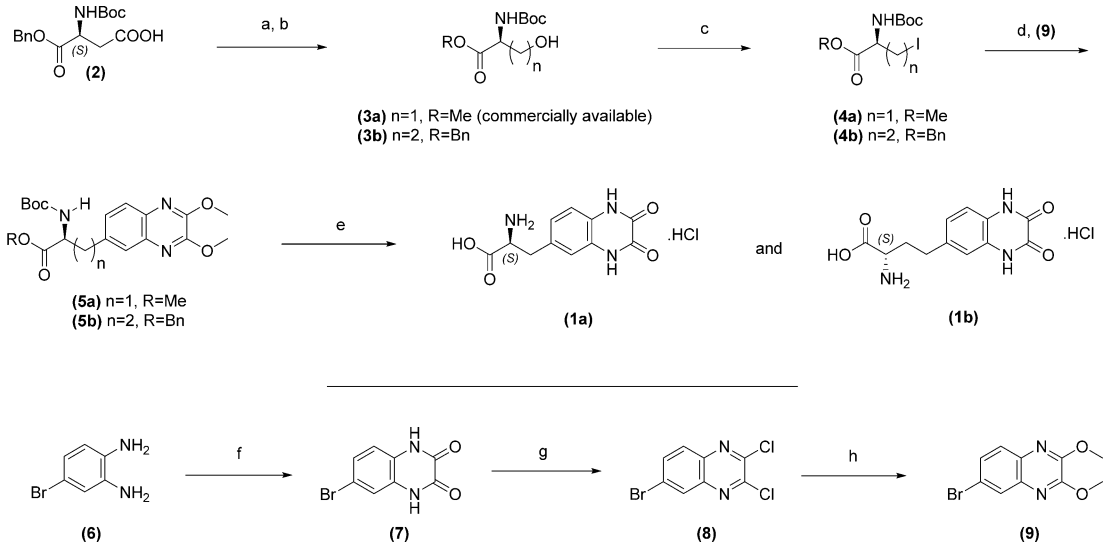

[a]Reagents and conditions: (a) *N*-methylmorpholine, isobutyl chloroformate, THF; (b) $NaBH_4$, MeOH; (c) PPh_3, imidazole, I_2, DCM (80% for R = Me, 49% over two steps for R = Bn); (d) Zn dust, I_2, Pd_2dba_3, SPhos, **9**, DMF (41% for R = Me, 35% for R = Bn); (e) 4 N HCl, H_2O, dioxane for **1a** (89%), recrystallization with propylene oxide for **1b** (68%); (f) diethyl oxalate (96%); (g) thionyl chloride, DMF (catalytic) (90%); (h) MeOK, MeOH (93%).

DOI: 10.1021/acschemneuro.5b00038
ACS Chem. Neurosci. XXXX, XXX, XXX−XXX

selective for GluK1 and ATPO binds to the GluK1 and AMPA receptors.

Functional Characterization at GluK1 and GluK2. We characterized the functionality of **1a** and **1b** at recombinantly expressed KA receptors. Outside-out patches excised from HEK293T cells transfected with GluK1 or GluK2 were subjected to fast Glu applications (250 ms, 1 mM Glu) in the absence or presence of 100 μM **1a** or **1b**, and peak currents were measured (Figure 4) and are summarized in Table 2.

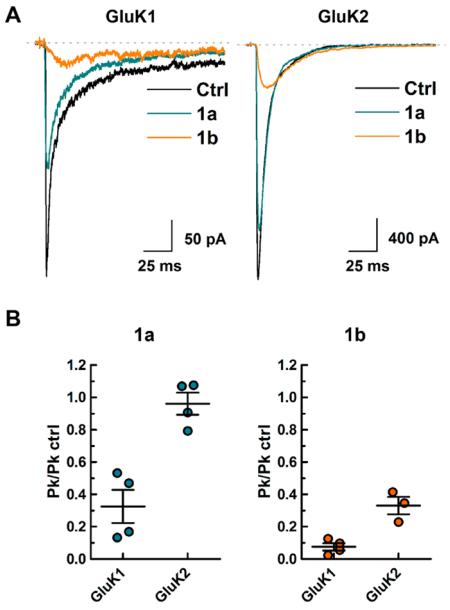

Figure 4. Antagonism of GluK1 and GluK2 by **1a** and **1b**. (A) Example GluK1 and GluK2 responses evoked by 1 mM Glu (patches 141215p2 and 141201p1, respectively) under control conditions (black) and in the presence of 100 μM **1a** (cyan) or **1b** (orange). (B) Summary of relative peak responses of GluK1 and GluK2 in the presence of 100 μM **1a** (left) or **1b** (right). Data points represent individual observations; lines and error bars represent the mean and SEM.

Table 2. Mean Relative Peak Responses Evoked by 1 mM Glu in the Presence of 100 μM 1a or 1b

	GluK1			GluK2		
	mean	SEM	*n*	mean	SEM	*n*
1a (CNG-10301)	0.33	±0.10	4	0.96	±0.07	4
1b (CNG-10300)	0.08	±0.02	4	0.33	±0.05	3

Surprisingly, 100 μM **1a** partially blocked GluK1, while GluK2 was unaffected (Figure 4B). On the other hand, **1b** fully antagonized GluK1 but only partially blocked GluK2 (Figure 4B). Of note, **1b** also slowed the rise time of both GluK1 and GluK2 responses by almost 13- and 6-fold, respectively (GluK1, 0.60 ± 0.08 and 7.8 ± 4.5 ms in control and **1b**, respectively; GluK2, 0.96 ± 0.05 and 5.6 ± 0.3 ms in control and **1b**, respectively). This is consistent with **1b** being a competitive antagonist at both GluK1 and GluK2 receptors.

We also investigated **1a** as a potential agonist at GluK1 and GluK2. At a concentration of 100 μM, **1a** alone did not produce any response at either GluK1 (n = 3) or GluK2 (n = 5) at a holding potential of −100 mV. Moreover, preliminary experiments using Concanavalin-A to enhance small agonist responses, as previously described,[21] did not change this outcome. On the basis of these results, we conclude that within the resolution of our system, **1a** is an antagonist and not a partial agonist at GluK1.

X-ray Structure of the GluK1-LBD with 1b. Today, approximately 300 structures of LBDs of iGluRs have been determined. Such high-resolution structures (1−2.5 Å) are valuable for gaining detailed information about ligand binding and hydrogen bonding, including binding site water networks. For comparison, structures of full-length GluA2 have been crystallized with three agonists and one antagonist only at medium to low resolution (3.2−3.9 Å).[22−24] However, a similar binding mode of the ligands as well as similar domain and subunit arrangements at the soluble LBD and full-length receptors was seen, which supports the use of LBDs for detailed studies.

Of compounds **1a** and **1b**, only **1b** was successfully crystallized with the GluK1-LBD at 2.28 Å resolution. The crystal contains three molecules (A−C) in the asymmetric unit of the crystal (Table S1 of the Supporting Information). Molecules A and C form a biologically relevant dimer with each other, whereas molecule B forms a dimer with a symmetry-related molecule B. Compound **1b** was found to bind with a similar binding affinity at the GluK1-LBD (37 μM) and at cloned homomeric GluK1 receptors (16 μM) (Table 1).

Compound **1b** could unambiguously be located at the three binding sites (Figure 5A−C). The ligand is positioned in such a way that the quinoxaline-2,3-dione part of **1b** forms contacts to the essential Arg523, in the same manner as seen in the structure of the GluA2-LBD with DNQX.[12] In this way, the α-amino acid moiety of **1b** can be regarded as a substituent on the quinoxaline-2,3-dione skeleton. The contacts to the quinoxaline-2,3-dione part of **1b** involve polar interactions between both oxygen atoms of **1b** and the Arg523 side chain as well as an interaction from the 2-one of **1b** to the backbone nitrogen atom of Thr518. Furthermore, the 3-one atom forms a contact with a water molecule in molecule B (Figure 5B), which is not seen in molecule A or C (Figure 5A,C). The 1-nitrogen atom of **1b** forms a contact with the backbone carbonyl oxygen atom of Pro516, whereas the 4-nitrogen atom interacts with a water molecule in molecules A and B. The side chain of Glu738 is twisted away from the ligand (Figure 5D) as previously also observed upon binding of UBP318 in the GluK1-LBD,[15] but in contrast to what was seen in other structures of GluK1 with antagonists, e.g., GluK1-LBD in complex ATPO,[14] where this residue forms direct contacts with the ligand (Figure 5D).

As GluK1 is an α-amino acid-binding receptor, a binding mode positioning the α-amino acid of **1b** toward Arg523 was predicted as one of the possible binding modes (see section on *In silico* study in the Supporting Information), and Glu738 was thought to bind to the ligand α-amino group of **1b**. Instead, the structure reveals that the α-amino acid moiety of **1b** binds in a small cavity inside the binding pocket (Figures 5D and 6). The *in silico* study showed that only when docking back into the **1b**−GluK1-LBD X-ray structure could the X-ray-determined binding mode of **1b** be reproduced. Following the concept of induced fit of ligand−protein binding, this is however not unexpected as three key parameters in this process are difficult to model: (1) receptor domain closure, (2) organization of water matrix and hydrogen bonding network in the binding pocket, and (3) overall entropy of the system whether this is positively or negatively contributing to the total free energy of binding.

DOI: 10.1021/acschemneuro.5b00038
ACS Chem. Neurosci. XXXX, XXX, XXX−XXX

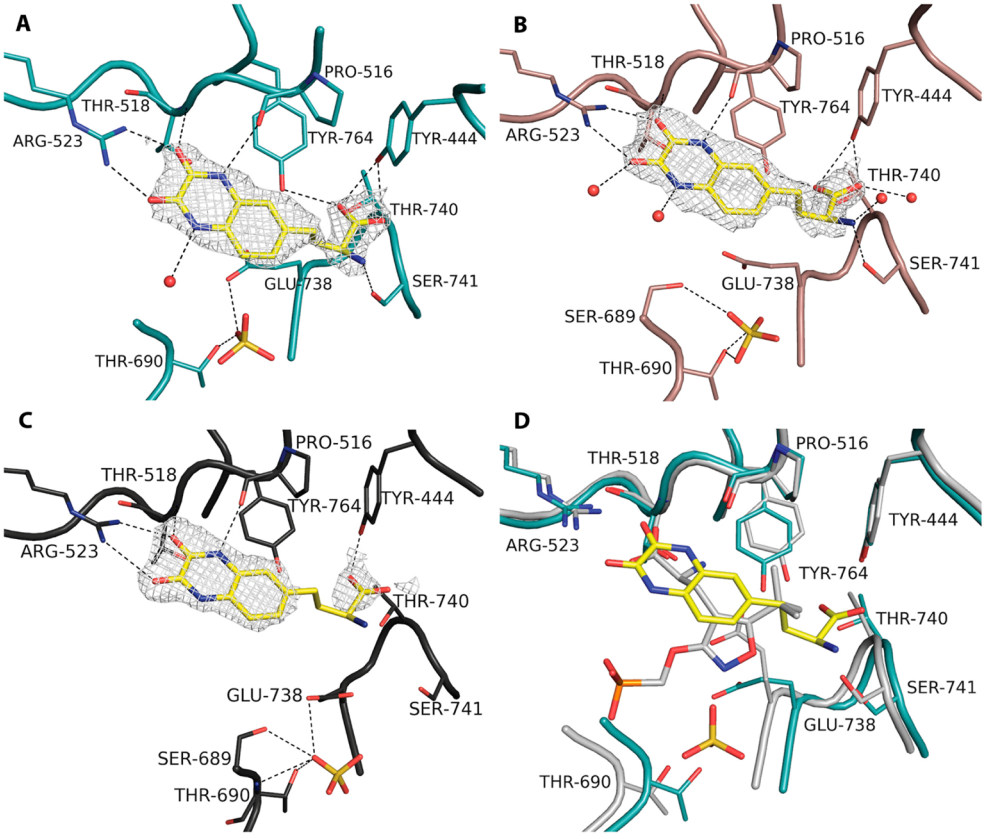

Figure 5. X-ray crystal structure of **1b** in the LBD of GluK1. (A–C) **1b** is shown as sticks with carbon atoms colored yellow. Selected binding site residues are illustrated with carbon atoms colored cyan (molecule A), salmon (molecule B), and dark gray (molecule C). The backbone trace is shown as a ribbon. Oxygen atoms are colored red, nitrogen atoms blue, and sulfur atoms yellow. Water molecules are displayed as red spheres, and a sulfate ion located in the binding site is shown as sticks. Potential hydrogen bonds within 3.2 Å are shown as dashed lines. Furthermore, a standard Phenix $2F_o - F_c$ omit map (gray) carved around the ligand at a 1.6 Å radius is shown: molecules (A) A, (B) B, and (C) C. (D) Superimposition of the structures of the GluK1-LBD with **1b** (molecule A, color coding as in panel A) and the GluK1-LBD with ATPO (PDB entry 1VSO,[14] molecule A, carbon atoms colored light gray). See Figure S1 of the Supporting Information for the final $2F_o - F_c$ electron density map of the three molecules of **1b**.

The α-amino group of **1b** in molecules A and B makes contacts with the side chain hydroxyl group of Ser741 and also a water molecule in molecule B (Figure 5A,B), whereas no close contacts with the α-amino group are seen in molecule C (Figure 5C). The α-carboxylate group of **1b** forms contacts with side chain hydroxyl groups of Tyr444, Thr740, and Tyr764 as well as a water molecule in molecule B. In molecule C, a close contact with Tyr444 (2.6 Å) is seen, whereas the contacts with Thr740 (3.6 Å) and Tyr764 (3.6 Å) are weaker. A sulfate ion is found in the binding pocket, which is located 6–8 Å from **1b** in the vicinity of Thr690 (Figure 5A–C) and forms similar contacts in all three molecules. Upon comparison of the present structure with the structure of the GluK1-LBD in complex with other antagonists, it is seen that a distal substituent of most antagonists is positioned where the sulfate ion is located in the structure of the GluK1-LBD with **1b** (Figure 6). The sulfate ion is found in a similar region as the phosphonate group of ATPO in the GluK1-LBD but in a different location (Figure 5D). In the structures of the GluA2-LBD with DNQX and NS1209, a sulfate ion is positioned at the same site as the phosphonate group of ATPO in the GluA2-LBD.[25] However, the phosphonate group of ATPO adopts different locations in the GluA2-LBD and GluK1-LBD[14] and also different from the sulfate ion in the GluK1-LBD structure with **1b**. Therefore, it seems that incorporation of an anionic moiety into a compound would favor binding at both GluA2 and GluK1 but may result in different receptor contacts.

Whereas agonists induce a closure of domain D2 toward domain D1, antagonists stabilize an open form of the LBD. D1–D2 domain openings were calculated for molecules A–C of the GluK1-LBD structure with antagonist **1b** bound using the GluK1-LBD structure with glutamate (PDB entry 2F36, molecule A)[26] as a reference structure. The domain opening of the three molecules was seen to be significantly different (25.4°, 29.0°, and 49.3° for molecules A–C, respectively) (Figure 7). Domain openings of GluK1-LBD have previously been found to vary from 25° to 31°.[15] Therefore, the domain opening of 49° in molecule C in the structure presented here is surprisingly large but at the same time demonstrates that the GluK1-LBD is capable of undergoing major domain movements. In the crystal, the entrances to the binding sites of molecules B and C are facing each other, and thus, this crystal packing might affect closure of molecule C. Also, the average *B* value (55 Å^2) of D2 in molecule C is significantly larger than those of the three D1 domains and the other two D2 domains in the structure (35–39 Å^2). This observation indicates high flexibility of domain D2 in molecule C, consistent with a large domain opening and weaker contacts of **1b** in molecule C compared to in molecules A and B.

DOI: 10.1021/acschemneuro.5b00038
ACS Chem. Neurosci. XXXX, XXX, XXX–XXX

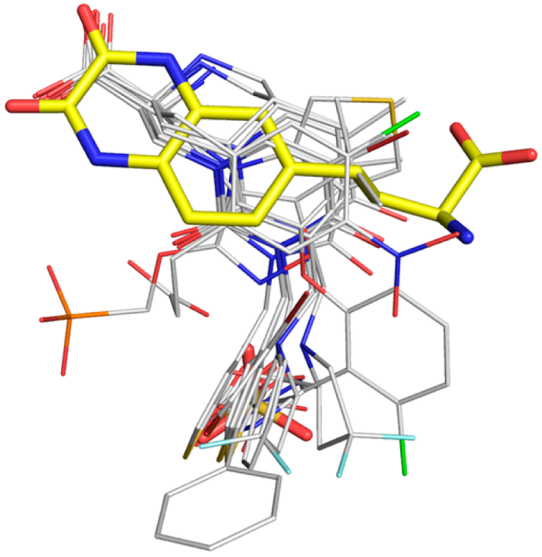

Figure 6. Superimposition on domain D1 of all 10 available antagonist structures at rat GluK1-LBD (molecule A) to illustrate that the amino acid part of **1b** points into an area of the binding pocket that has not previously been explored by antagonists. All reported antagonists have substituents pointing in the direction of the sulfate ion. Only ligand atoms are shown for the sake of clarity (yellow sticks, **1b** and sulfate ion; thin gray lines, PDB entries 1VSO, 2F34, 2F35, 2QS1, 2QS2, 2QS3, 2QS4, 3S2V, 4DLD, and 4MF3).

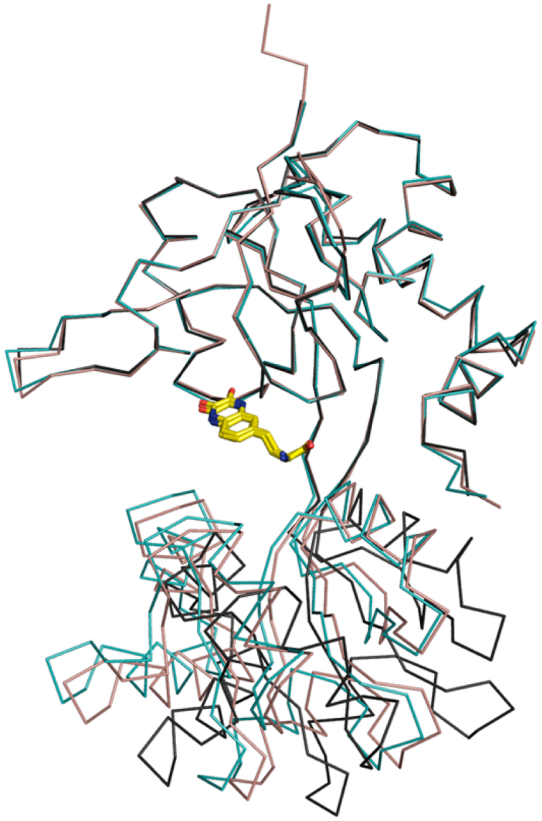

Figure 7. Molecules A−C of the GluK1-LBD structure with **1b** superimposed on domain D1 residues. Molecule A is colored cyan, molecule B salmon, and molecule C dark gray. **1b** is shown as yellow sticks.

Crystallization of **1b** with the GluA2-LBD was also attempted. The diffraction data showed the GluA2 LBD to be in an open cleft conformation; however, a lack of interpretable electron density in the binding site prevented modeling of **1b** into the structure (data not shown). On the basis of a comparison of amino acid residues in the GluK1-LBD and GluA2-LBD, only one difference is seen within 4 Å of **1b**: Ser741 in GluK1, which corresponds to a methionine in GluA2 (Met708). The α-amino group in **1b** forms a hydrogen bond with the side chain hydroxyl group of Ser741 in GluK1 (Figure 5). Thus, this hydrogen bond is not possible in the GluA2-LBD and might suggest a different binding mode of **1b** in GluA2 compared to that in GluK1. However, it has been observed that Met708 in GluA2 can undergo major side chain conformational changes,[27] and therefore, the α-amino acid substituent might point into a similar region in GluA2 as observed for GluK1. This would be in agreement with a similar binding affinity of **1b** in GluA2 and GluK1 (Table 1).

CONCLUSION

Discovery of iGluR antagonists that display an unprecedented receptor subtype selectivity profile continues to be a challenging task. By means of creativity together with structural insight into the iGluRs and the binding modes of their ligands, amino acid-functionalized quinoxalines **1a** (CNG-10301) and **1b** (CNG-10300) were designed and successfully synthesized. Analogue **1a** displayed midrange micromolar affinity for the GluK2 subtype and low affinity for GluK1 and GluK3. However, in a functional setup, **1a** antagonized GluK1 but not GluK2 (33 and 96% peak responses at 100 μM, respectively). Analogue **1b** showed binding affinities for native AMPA, KA, and NMDA and the three GluK1−3 subtypes in the low to medium micromolar range. At 100 μM, **1b** fully antagonized GluK1 and partially antagonized GluK2. An X-ray crystal structure of the GluK1-LBD with **1b** revealed an unexpected binding mode and a large variation in domain openings of the three molecules from 25° to 49°, demonstrating that the GluK1-LBD is capable of undergoing major domain movements.

In all, the new insight presented herein is valuable for the future design and synthesis of subtype-selective iGluR antagonists.

EXPERIMENTAL SECTION

Chemistry. All reactions involving dry solvents or sensitive agents were performed under a nitrogen atmosphere, and glassware was dried prior to use. Commercially available chemicals were used without further purification. THF and DMF were dried using 3 Å molecular sieves. Reactions were monitored by analytical thin-layer chromatography (TLC, Merck silica gel 60 F_{254} aluminum sheets). Flash chromatography was conducted using Merck silica gel 60A (20−45 μm). ^{1}H NMR spectra were recorded on a 300 MHz Avance Bruker spectrometer and ^{13}C NMR spectra on a 75 MHz Avance Bruker spectrometer. The purity of all tested compounds was determined by elementary analysis to be >95%.

(*S*)-Benzyl 2-[(*tert*-Butoxycarbonyl)amino]-4-hydroxybutanoate (3b). To a solution of (*S*)-4-(benzyloxy)-3-[(*tert*-butoxycarbonyl)amino]-4-oxobutanoic acid **2** (2.00 g, 6.18 mmol) in dry THF (30 mL) at −15 °C was added *N*-methylmorpholine (0.680 mL, 6.18 mmol) followed by isobutyl chloroformate (0.810 mL, 6.18 mmol) (milky solution). The solution was stirred for 20 min, and $NaBH_4$ (0.700 g, 18.5 mmol) was added portionwise followed by a slow dropwise addition of MeOH (62 mL) over 45 min. The reaction mixture was stirred for 40 min at −15 °C before the reaction was quenched by the addition of an aqueous solution of HCl (11 mL, 1 M). The mixture was concentrated under reduced pressure, and the residue was extracted with EtOAc (3 × 30 mL). The combined

DOI: 10.1021/acschemneuro.5b00038
ACS Chem. Neurosci. XXXX, XXX, XXX−XXX

organic layers were successively washed with an aqueous solution of HCl (1 × 40 mL, 1 M), H_2O (2 × 50 mL), an aqueous solution of 5% $NaHCO_3$ (1 × 50 mL), and finally H_2O (3 × 50 mL). It was dried over $MgSO_4$, filtered, and evaporated under reduced pressure, leading to a yellow oil. The crude was used without purification.

General Procedure for the Displacement of the Primary Hydroxy Group with Iodine. To a solution of PPh_3 (2.02 g, 7.70 mmol) and imidazole (0.520 g, 7.70 mmol) in DCM (29 mL) at 0 °C was added I_2 (1.95 g, 7.70 mmol) (orange milky solution). The reaction mixture was warmed to room temperature and stirred for 10 min. The mixture was recooled to 0 °C, and a solution of the corresponding alcohol (6.16 mmol) in DCM (6 mL) was added dropwise over 15 min. The solution was stirred at 0 °C for 90 min and then at room temperature for 2 h. The reaction mixture was filtered off through a pad of Celite (2 cm) using a solution of ether and petroleum ether (1:1) as the eluent. The organic phase was evaporated under reduced pressure without being heated.

*(S)-Methyl 2-[(tert-Butoxycarbonyl)amino]-3-iodopropanoate (**4a**).* Purified by flash column chromatography (ether/petroleum ether, 1:4) (R_f = 0.19). White solid (2.85 g, 80%). Mp: 51 °C (Lit. 51 °C). ^{1}H NMR (300 MHz, $CDCl_3$): δ 5.34 (d, J = 7.06 Hz, 1H), 4.55−4.47 (m, 1H), 3.79 (s, 3H), 3.62−3.50 (m, 2H), 1.45 (s, 9H).

*(S)-Benzyl 2-[(tert-Butoxycarbonyl)amino]-4-iodobutanoate (**4b**).* Purified by flash column chromatography (EtOAc/petroleum ether, 1:5) (R_f = 0.5). White solid (1.3 g, 49% over two steps). Mp: 54 °C (Lit. 54 °C). ^{1}H NMR (300 MHz, $CDCl_3$): δ 7.39−7.32 (m, 5H), 5.22 (dd, J = 2.91 Hz, 1H), 5.13−5.03 (m, 1H), 4.41−4.35 (m, 1H), 3.21−3.08 (m, 2H), 2.41−2.35 (m, 1H), 2.25−2.17 (m, 1H), 1.45 (s, 9H).

General Procedure for the Negishi Cross Coupling Reaction. Zinc dust (0.61 g, 9.30 mmol) was added to a nitrogen-purged vial. Dry DMF (3.25 mL) was added followed by a catalytic amount of I_2 (40 mg, 0.15 mmol) (the solution turned yellow and then black again). The corresponding iodine compound, **4a** or **4b** (3.10 mmol), was immediately added followed by another catalytic amount of I_2 (40 mg, 0.15 mmol) (the solution turned yellow-green and then black again; exothermicity was felt because of zinc insertion). Pd_2dba_3 (73 mg, 0.08 mmol), SPhos (62 mg, 0.150 mmol), and 6-bromo-2,3-dimethoxyquinoxaline **9** (0.290 g, 1.08 mmol) were added to the vial, and the solution was heated at 50 °C for 4 h. The reaction mixture was filtered off through a pad of Celite (2 cm), washed with DMF, and evaporated under reduced pressure. Water (10 mL) was added, and the solution was extracted with Et_2O (3 × 20 mL). Combined organic phases were washed with brine, dried over $MgSO_4$, filtered, and evaporated under reduced pressure.

*(S)-Methyl 2-[(tert-Butoxycarbonyl)amino]-3-(2,3-dimethoxyquinoxalin-6-yl)propanoate (**5a**).* Purified twice by flash column chromatography [AcOEt/heptane, 3:7 (R_f = 0.30), and then toluene/AcOEt, 85:15 (R_f = 0.35)]. White solid (0.5 g, 41%). Mp: 56.4 °C. $[\alpha]_D^{25}$ = +67.5 (c = 0.306 g/100 mL, CH_2Cl_2). ^{1}H NMR (300 MHz, $CDCl_3$): δ 7.69 (d, J = 8.34 Hz, 1H), 7.55 (br s, 1H), 7.26 (dd, J = 8.33, 1.98 Hz, 1H), 5.02 (d, J = 7.99 Hz, 1H), 4.66 (dd, J = 13.73, 6.05 Hz, 1H), 4.14 (s, 6H), 3.74 (s, 3H), 3.24 (dq, J = 13.97, 6.07 Hz, 2H), 1.42 (9H, s). ^{13}C NMR (75 MHz, $CDCl_3$): δ 172.1, 154.9, 149.9, 149.7, 136.9, 136.1, 134.6, 127.8, 126.7, 126.3, 79.9, 54.4, 54.1, 52.2, 38.1, 28.2.

*(S)-Benzyl 2-[(tert-Butoxycarbonyl)amino]-4-(2,3-dimethoxyquinoxalin-6-yl)butanoate (**5b**).* Purified four times by flash column chromatography [twice with EtOAc/heptane, 3:7 (R_f = 0.33), then DCM/MeOH (5%) (R_f = 0.38), and then toluene/EtOAc, 9:1 (R_f = 0.30)]. Orange glass solid (1.0 g, 35%). Mp: 67.6 °C. $[\alpha]_D^{25}$ = +22.0 (c = 0.4 g/100 mL, CH_2Cl_2). ^{1}H NMR (300 MHz, $CDCl_3$): δ 7.65 (d, J = 8.35 Hz, 1H), 7.52 (br s, 1H), 7.38−7.34 (m, 4H), 7.26 (s, 1H), 7.26−7.15 (m, 1H), 5.16 (dd, J = 19.42, 12.28 Hz, 2H), 5.14 (br s, 1H), 4.44 (dd, J = 12.99, 7.03 Hz, 1H), 4.14 (s, 6H), 2.88−2.67 (m, 2H), 2.34−2.15 (m, 1H), 2.10−1.95 (m, 1H), 1.46 (s, 9H). ^{13}C NMR (75 MHz, $CDCl_3$): δ 172.3, 155.2, 149.8, 149.5, 139.4, 137.0, 135.5, 135.2, 128.5, 128.3, 128.2, 127.4, 126.2, 125.4, 79.9, 67.0, 54.0, 53.2, 34.2, 31.3, 28.2.

*(S)-2-Amino-3-(2,3-dioxo-1,2,3,4-tetrahydroquinoxalin-6-yl)-propanoic Acid Hydrochloride (**1a**).* To a solution of (*S*)-methyl 2-[(*tert*-butoxycarbonyl)amino]-3-(2,3-dimethoxyquinoxalin-6-yl)-propanoate **5a** (0.400 g, 1.02 mmol) in dioxane (19 mL) was added an aqueous solution of HCl (19 mL, 4 N), and the reaction mixture was heated under gentle reflux conditions overnight. The reaction mixture was evaporated, and the residue was triturated with Et_2O (3 × 5 mL), leading to a pure white HCl salt (250 mg, 89%). Mp: 278 °C dec. $[\alpha]_D^{25}$ = +48.0 (c = 0.167 g/100 mL, DMSO). ^{1}H NMR (300 MHz, d_6-DMSO): δ 12.00 (s, 1H), 11.95 (s, 1H), 8.33 (br s, 3H), 7.07 (d, J = 8.60 Hz, 1H), 7.01−6.96 (m, 2H), 4.08 (br s, 1H), 3.07 (d, J = 6.42 Hz, 2H). ^{13}C NMR (75 MHz, d_6-DMSO): δ 170.1, 155.1, 154.9, 129.7, 125.5, 124.7, 124.2, 116.1, 115.3, 53.2, 35.2. Anal. Calcd for $C_{12}H_{13}N_3O_4{\cdot}0.34H_2O{\cdot}1.62HCl$): C, 43.88; H, 4.7; N, 12.79. Found: C, 43.58; H, 4.38; N, 13.12.

*(S)-2-Amino-4-(2,3-dioxo-1,2,3,4-tetrahydroquinoxalin-6-yl)-butanoic Acid Hydrochloride (**1b**).* To a solution of (*S*)-benzyl 2-[(*tert*-butoxycarbonyl)amino]-4-(2,3-dimethoxyquinoxalin-6-yl)-butanoate **5b** (0.250 g, 0.52 mmol) in dioxane (12 mL) was added an aqueous solution of HCl (12 mL, 4 N), and the solution was heated under gentle reflux conditions overnight. The reaction mixture was then evaporated, and the residue was triturated with Et_2O (3 × 5 mL). The crude was obtained as a light orange powder (96%).

The crude (150 mg, 0.5 mmol) was dissolved in H_2O (8 mL) and the mixture stirred at room temperature. Propylene oxide (35 μL, 5.0 mmol) was slowly added to the reaction mixture, and the solution was stirred for 30 min. The reaction mixture was left overnight without stirring for crystallization and then filtered with a filter paper, and crystals were washed with H_2O (3 × 2 mL). The crystals were dissolved in an aqueous solution of HCl (1.5 mL, 1 M) and evaporated to dryness. The solid was dissolved in H_2O (2 mL) and freeze-dried to afford a light brown solid (106 mg, 68%). Mp: 263 °C dec. $[\alpha]_D^{25}$ = +35.8 (c = 0.142 g/100 mL, H_2O). ^{1}H NMR (300 MHz, d_6-DMSO): δ 11.95 (s, 1H), 11.91 (s, 1H), 8.48 (br s, 3H), 7.07 (d, J = 7.97 Hz, 3H), 6.95 (br s, 1H), 6.94 (br dd, J = 9.13, 1.48 Hz, 1H), 3.87 (signal hidden by the solvent peak, 1H), 2.82−2.67 (m, 1H), 2.67−2.53 (m, 1H), 2.10−1.96 (m, 2H). ^{1}H NMR (300 MHz, D_2O): δ 7.00 (ddd, J = 8.27, 1.68, 1.68 Hz, 1H), 6.94 (dd, J = 8.31, 1.51 Hz, 1H), 6.87 (br d, J = 1.39 Hz, 1H), 3.99 (dd, J = 6.25, 6.25 Hz, 1H), 2.81−2.55 (m, 2H), 2.13−1.99 (m, 2H). ^{13}C NMR (75 MHz, d_6-DMSO): δ 170.7, 155.3, 155.0, 135.4, 125.6, 124.0, 123.1, 115.3, 114.6, 51.6, 32.0, 30.0. Anal. Calcd for $C_{12}H_{14}ClN_3O_4{\cdot}1.5H_2O{\cdot}0.81HCl$): C, 40.84; H, 4.67; N, 11.41. Found: C, 40.46; H, 5.04; N, 11.79.

*6-Bromoquinoxaline-2,3(1H,4H)-dione (**7**).* A solution of 2-amino-4-bromoaniline **6** (3.0 g, 16.0 mmol) in diethyl oxalate (15 mL) was refluxed for 4 h. The reaction mixture was allowed to cool to room temperature, after which EtOAc (25 mL) was added. The precipitate was filtered and washed with EtOAc (3 × 20 mL) and dried under vacuum to give a brown powder (3.75 g, 96%). ^{1}H NMR (300 MHz, d_6-DMSO): δ 11.97 (s, 1H), 11.94 (s, 1H), 7.26−7.18 (m, 2H), 7.03 (d, J = 9.03 Hz, 1H). Mp: >400 °C dec (Lit. >350 °C).

*6-Bromo-2,3-dichloroquinoxaline (**8**).* To a mixture of 6-bromoquinoxaline-2,3(1*H*,4*H*)-dione **7** (5.33 g, 22.11 mmol) in thionyl chloride (74 mL) was added a catalytic amount of DMF (three drops). The reaction mixture was heated under reflux for 8 h, cooled to room temperature, and poured very slowly into an ice/water bath. The solid was filtered, dissolved in EtOAc (500 mL), and dried with $MgSO_4$. The organic phase was filtered and evaporated to afford the desired product, 6-bromo-2,3-dichloroquinoxaline **8**, as a light orange-brown solid (1.03 g, 90%). Mp: 131 °C (Lit. 132 °C). ^{1}H NMR (300 MHz, d_6-DMSO): δ 8.34 (d, J = 2.01 Hz, 1H), 8.05 (dd, J = 8.91, 2.06 Hz, 1H), 8.00 (d, J = 8.89 Hz, 1H).

*6-Bromo-2,3-dimethoxyquinoxaline (**9**).* To a solution of the intermediate 6-bromo-2,3-dichloroquinoxaline **8** (2.25 g, 8.09 mmol) in anhydrous methanol (34 mL) was added a solution of 25% MeOK in MeOH (6.90 mL, 22.6 mmol). The reaction mixture was refluxed for 3 h and cooled to room temperature. H_2O (50 mL) was added, and the suspension was filtered before being washed with water (3 × 20 mL). The solid was dried overnight using a vacuum oven to give the desired product, 6-bromo-2,3-dimethoxyquinoxaline **9**, as a brown powder (2.02 g, 93%). Mp: 105 °C (Lit. 114−115 °C, solvent of

DOI: 10.1021/acschemneuro.5b00038
ACS Chem. Neurosci. XXXX, XXX, XXX−XXX

methanol). ^{1}H NMR (300 MHz, d_6-DMSO): δ 7.90 (br s, 1H), 7.67 (d, J = 9.09 Hz, 1H), 7.63 (d, J = 8.77 Hz, 1H), 4.03 (s, 6H).

Pharmacology. Radioligand displacement studies were performed as previously described at native rat brain AMPA, KA, and NMDA receptors and at recombinant rat homomeric GluA2(R)$_o$, GluK1(Q)$_{1b}$, GluK2(VCR)$_a$, and GluK3$_a$ receptors as well as the GluK1-LBD.[28] For recombinant kainate receptor assays, [^{3}H]SYM2081 was used as the radioligand while [^{3}H]AMPA was employed for the GluA2(R)$_o$ binding assay.

Cell Culture and Transfection. HEK293T/17 cells (ATCC) were maintained in minimal essential medium (MEM) containing glutaMAX supplemented with 10% fetal bovine serum (Invitrogen). Cells were plated at a low density (1.6−2.0 × 10^4 cells/mL) on poly-D-lysine-coated 35 mm plastic dishes and were transiently transfected 24 h later using the calcium phosphate technique as previously described.[29] Rat cDNA encoding for GluK1−2a and GluK2a subunits was cotransfected with cDNA encoding enhanced green fluorescent protein (eGFP) to identify transfected cells.

Electrophysiological Recordings. Experiments were performed 36−48 h after transfection. Agonist solutions were rapidly applied to outside-out patches excised from transfected cells using a piezoelectric stack (Physik Instrumente). Solution exchange (10−90% rise time of 250−350 μs) was determined in a separate experiment by measuring the liquid junction current. All recordings were performed using an Axopatch 200B (Molecular Devices) using thick-walled borosilicate glass pipettes (3−6 MΩ) coated with dental wax to reduce electrical noise. Current records were filtered at 5 kHz, digitized at 25 kHz, and series resistance (3−12 MΩ) compensated by 95%. Recordings were performed at a holding potential of −100 mV. All experiments were performed at room temperature. All chemicals used for electrophysiology were purchased from Sigma-Aldrich unless otherwise indicated. The external solution contained 150 mM NaCl, 5 mM HEPES, 0.1 mM $MgCl_2$, and 0.1 mM $CaCl_2$ (pH 7.3−7.4). The internal solution contained 115 mM NaCl, 10 mM NaF, 5 mM HEPES, 5 mM Na_4BAPTA (Life Technologies), 1 mM $MgCl_2$, 0.5 mM $CaCl_2$, and 10 mM Na_2ATP (pH 7.3−7.4). The osmotic pressure of all solutions was adjusted to 295−300 mOsm with sucrose. Concentrated (100×) L-Glu stocks were prepared and stored at −20 °C; stocks were thawed and diluted on the day of the experiment. Concentrated (3 mM in DMSO) stocks of **1a** and **1b** were prepared and stored at −20 °C; stocks were thawed on the day of the experiment and added to the control and agonist external solutions for a final concentration of 100 μM. As a control, an equivalent amount of DMSO was added to the external solutions not containing **1a** or **1b**. To test whether **1a** was a partial agonist at GluK1 and GluK2 receptors, 100 μM **1a** was applied to outside-out patches alone. The presence of receptors in the patch was confirmed by obtaining a response with 1 mM L-Glu. The plant lectin, Concanavalin-A, was dissolved at ∼1 mg/mL in an external solution and applied to the patch for 1−2 min. Data were acquired using pClamp10 software (Molecular Devices) and tabulated using Excel (Microsoft Corp.).

X-ray Structure Determination. The rat GluK1-LBD (GRIK1_RAT, UNP P22756, segment S1 residues 430−544 and segment S2 residues 667−805) was expressed and purified in the presence of Glu as previously described.[30] Crystallization of GluK1-LBD in complex with **1b** was performed using the hanging drop vapor diffusion method at 6 °C. A protein solution consisting of 5 mg/mL GluK1-LBD, 5.2 mM **1b**, 10 mM HEPES, 20 mM NaCl, and 1 mM EDTA (pH 7.0) was prepared and used for crystallization experiments. Crystals used for diffraction studies were obtained under the following conditions: 24.4% PEG4000, 0.3 M ammonium sulfate, and 0.1 M phosphate citrate buffer (pH 4.5). The crystals were flash-cooled with liquid nitrogen after immersion in cryo buffer (1 μL of reservoir solution containing 1 μL of UCP). Flash-cooled crystals were stored in liquid nitrogen until data were collected.

An X-ray diffraction data set to 2.28 Å resolution was collected on beamline I911-3 at MAX-lab (Lund, Sweden). The data were processed with XDS[31] and scaled using SCALA[32] in CCP4i.[33] The structure was determined by molecular replacement using PHASER[34] within CCP4i and the structure of the GluK1-LBD in complex with (S)-ATPO as a search model (PDB entry 1VSO, molecule A; protein atoms only).[14] The search model was defined as two domains, D1 and D2. Three molecules were found in the asymmetric unit of the crystal. Visual inspection of the structure in COOT[35] revealed well-defined electron density for the structure in most areas and clear density corresponding to **1b**. The ligand coordinates were created in Maestro (Maestro version 9.2, Schrödinger, LLC, New York, NY) and fit into the electron density. Topology and parameter files for **1b** were obtained using eLBOW.[36] The model used for molecular replacement lacked two loops (residues 493−497 and 712−714), and these residues were built in manually. The structure was refined in PHENIX[37] with isotropic B factors and validated using tools in COOT and PHENIX. The final structure was also validated on the PDB ADIT validation server. Statistics of data collection and refinement can be found in Table S1 of the Supporting Information. D1−D2 domain openings were calculated using the DynDom server.[38]

***In Silico* Conformational Search Study.** Conformational searches and superimposition studies were performed using the software package MOE 2013.08 (Molecular Operating Environment, Chemical Computing Group). The built-in function "stochastic search" was used with the standard setup: mmff94x force field, solvation set to GB/SA, and energy cutoff of >7 kcal/mol.

■ ASSOCIATED CONTENT

Ⓢ Supporting Information

Crystal data, data collection, and refinement statistics of GluK1-LBD in complex with **1b** (Table S1), final 2Fo-Fc electron density of the three molecules of **1b** (Figure S1), and *in silico* study of the binding mode of **1b** (Table S2 and Figure S2). This material is available free of charge via the Internet at http://pubs.acs.org.

Accession Codes

The structure of the GluK1-LBD in complex with **1b** (CNG-10300) has been deposited in as Protein Data Bank entry 4QF9.

■ AUTHOR INFORMATION

Corresponding Authors

*Phone: +45 35336244. Fax: +45 35336041. E-mail: lebu@sund.ku.dk.

*E-mail: jsk@sund.ku.dk (for X-ray crystallography).

Author Contributions

C.S.D. (medicinal chemistry) and C.M. (X-ray crystallography) contributed equally to this work.

Funding

We thank the Lundbeck Foundation, the Carlsberg Foundation, The University of Copenhagen Programme of Excellence (GluTarget), the Hørslev Foundation, and Danscatt for financial support.

Notes

The authors declare no competing financial interest.

■ ACKNOWLEDGMENTS

Diffraction data were collected at the MAX-lab synchrotron facility in Lund, Sweden. Heidi Peterson is thanked for technical assistance.

■ ABBREVIATIONS

AMPA, α-amino-3-hydroxy-5-methyl-4-isoxazolepropionic acid; CNS, central nervous system; EAATs, excitatory amino acid transporters; Glu, (S)-glutamate; iGluRs, ionotropic Glu receptors; KA, kainic acid; LBD, ligand-binding domain; mGluRs, metabotropic Glu receptors; NMDA, *N*-methyl-D-aspartate

DOI: 10.1021/acschemneuro.5b00038
ACS Chem. Neurosci. XXXX, XXX, XXX−XXX

REFERENCES

(1) Anggono, V., and Huganir, R. L. (2012) Regulation of AMPA receptor trafficking and synaptic plasticity. *Curr. Opin. Neurobiol. 22*, 461−469.

(2) Lovinger, D. M. (2010) Neurotransmitter roles in synaptic modulation, plasticity and learning in the dorsal striatum. *Neuropharmacology 58*, 951−961.

(3) Jane, D. E., Lodge, D., and Collingridge, G. L. (2009) Kainate receptors: Pharmacology, function and therapeutic potential. *Neuropharmacology 56*, 90−113.

(4) Contractor, A., Mulle, C., and Swanson, G. T. (2011) Kainate receptors coming of age: Milestones of two decades of research. *Trends Neurosci. 34*, 154−163.

(5) Matute, C. (2011) Therapeutic Potential of Kainate Receptors: Therapeutic Potential of Kainate Receptors. *CNS Neurosci. Ther. 17*, 661−669.

(6) Ogden, K. K., and Traynelis, S. F. (2011) New advances in NMDA receptor pharmacology. *Trends Pharmacol. Sci. 32*, 726−733.

(7) Larsen, A. M., and Bunch, L. (2011) Medicinal Chemistry of Competitive Kainate Receptor Antagonists. *ACS Chem. Neurosci. 2*, 60−74.

(8) Weiss, B., Alt, A., Ogden, A. M., Gates, M., Dieckman, D. K., Clemens-Smith, A., Ho, K. H., Jarvie, K., Rizkalla, G., and Wright, R. A. (2006) Pharmacological characterization of the competitive GLUK5 receptor antagonist decahydroisoquinoline LY466195 in vitro and in vivo. *J. Pharmacol. Exp. Ther. 318*, 772−781.

(9) Randle, J. C., Guet, T., Cordi, A., and Lepagnol, J. M. (1992) Competitive inhibition by NBQX of kainate/AMPA receptor currents and excitatory synaptic potentials: Importance of 6-nitro substitution. *Eur. J. Pharmacol. 215*, 237−244.

(10) Poulie, C. B. M., and Bunch, L. (2013) Heterocycles as nonclassical bioisosteres of α-amino acids. *ChemMedChem 8*, 205−215.

(11) Hogner, A., Greenwood, J. R., Liljefors, T., Lunn, M.-L., Egebjerg, J., Larsen, I. K., Gouaux, E., and Kastrup, J. S. (2003) Competitive antagonism of AMPA receptors by ligands of different classes: Crystal structure of ATPO bound to the GluR2 ligand-binding core, in comparison with DNQX. *J. Med. Chem. 46*, 214−221.

(12) Armstrong, N., and Gouaux, E. (2000) Mechanisms for activation and antagonism of an AMPA-sensitive glutamate receptor: Crystal structures of the GluR2 ligand binding core. *Neuron 28*, 165−181.

(13) Cordi, A. A., Desos, P., Randle, J. C., and Lepagnol, J. (1995) Structure-activity relationships in a series of 3-sulfonylamino-2-(1H)-quinolones, as new AMPA/kainate and glycine antagonists. *Bioorg. Med. Chem. 3*, 129−141.

(14) Hald, H., Naur, P., Pickering, D. S., Sprogøe, D., Madsen, U., Timmermann, D. B., Ahring, P. K., Liljefors, T., Schousboe, A., and Egebjerg, J. (2007) Partial agonism and antagonism of the ionotropic glutamate receptor iGluR5 structures of the ligand-binding core in complex with domoic acid and 2-amino-3-[5-*tert*-butyl-3-(phosphonomethoxy)-4-isoxazolyl]propionic acid. *J. Biol. Chem. 282*, 25726−25736.

(15) Alushin, G. M., Jane, D., and Mayer, M. L. (2011) Binding site and ligand flexibility revealed by high resolution crystal structures of GluK1 competitive antagonists. *Neuropharmacology 60*, 126−134.

(16) Jackson, R. F., Moore, R. J., Dexter, C. S., Elliott, J., and Mowbray, C. E. (1998) Concise synthesis of enantiomerically pure phenylalanine, homophenylalanine, and bishomophenylalanine derivatives using organozinc chemistry: NMR studies of amino acid-derived organozinc reagents. *J. Org. Chem. 63*, 7875−7884.

(17) Ross, A. J., Lang, H. L., and Jackson, R. F. (2010) Much improved conditions for the Negishi cross-coupling of iodoalanine derived zinc reagents with aryl halides. *J. Org. Chem. 75*, 245−248.

(18) Broadrup, R. L., Wang, B., and Malachowski, W. P. (2005) A general strategy for the synthesis of azapeptidomimetic lactams. *Tetrahedron 61*, 10277−10284.

(19) Adamczyk, M., Johnson, D. D., and Reddy, R. E. (2000) A concise synthesis of (S)-(−)-3-(2-carboxy-4-pyrrolyl)-alanine. *Tetrahedron: Asymmetry 11*, 3063−3068.

(20) Jensen, A. A., and Braüner-Osborne, H. (2004) Pharmacological characterization of human excitatory amino acid transporters EAAT1, EAAT2 and EAAT3 in a fluorescence-based membrane potential assay. *Biochem. Pharmacol. 67*, 2115−2127.

(21) Fay, A.-M. L., Corbeil, C. R., Brown, P., Moitessier, N., and Bowie, D. (2009) Functional characterization and in silico docking of full and partial GluK2 kainate receptor agonists. *Mol. Pharmacol. 75*, 1096−1107.

(22) Sobolevsky, A. I., Rosconi, M. P., and Gouaux, E. (2009) X-ray structure, symmetry and mechanism of an AMPA-subtype glutamate receptor. *Nature 462*, 745−756.

(23) Yelshanskaya, M. V., Li, M., and Sobolevsky, A. I. (2014) Structure of an agonist-bound ionotropic glutamate receptor. *Science 345*, 1070−1074.

(24) Dürr, K. L., Chen, L., Stein, R. A., De Zorzi, R., Folea, I. M., Walz, T., Mchaourab, H. S., and Gouaux, E. (2014) Structure and dynamics of AMPA receptor GluA2 in resting, pre-open, and desensitized states. *Cell 158*, 778−792.

(25) Kasper, C., Pickering, D. S., Mirza, O., Olsen, L., Kristensen, A. S., Greenwood, J. R., Liljefors, T., Schousboe, A., Wätjen, F., Gajhede, M., Sigurskjold, B. W., and Kastrup, J. S. (2006) The structure of a mixed GluR2 ligand-binding core dimer in complex with (S)-glutamate and the antagonist (S)-NS1209. *J. Mol. Biol. 357*, 1184−1201.

(26) Mayer, M. L., Ghosal, A., Duolman, N. P., and Jane, D. E. (2006) Crystal structures of the kainate receptor GluR5 ligand binding core dimer with novel GluR5-selective antagonists. *J. Neurosci. 26*, 2852−2861.

(27) Pøhlsgaard, J., Frydenvang, K., Madsen, U., and Kastrup, J. S. (2011) Lessons from more than 80 structures of the GluA2 ligand-binding domain in complex with agonists, antagonists and allosteric modulators. *Neuropharmacology 60*, 135−150.

(28) Assaf, Z., Larsen, A. P., Venskutonytė, R., Han, L., Abrahamsen, B., Nielsen, B., Gajhede, M., Kastrup, J. S., Jensen, A. A., Pickering, D. S., Frydenvang, K., Gefflaut, T., and Bunch, L. (2013) Chemoenzymatic Synthesis of New 2,4-*syn*-Functionalized (*S*)-Glutamate Analogues and Structure−Activity Relationship Studies at Ionotropic Glutamate Receptors and Excitatory Amino Acid Transporters. *J. Med. Chem. 56*, 1614−1628.

(29) Maclean, D. M., Wong, A. Y. C., Fay, A.-M., and Bowie, D. (2011) Cations but not anions regulate the responsiveness of kainate receptors. *J. Neurosci. 31*, 2136−2144.

(30) Naur, P., Vestergaard, B., Skov, L. K., Egebjerg, J., Gajhede, M., and Kastrup, J. S. (2005) Crystal structure of the kainate receptor GluR5 ligand-binding core in complex with (S)-glutamate. *FEBS Lett. 579*, 1154−1160.

(31) Kabsch, W. (2010) XDS. *Acta Crystallogr. D66*, 125−132.

(32) Evans, P. (2006) Scaling and assessment of data quality. *Acta Crystallogr. D62*, 72−82.

(33) Winn, M. D., Ballard, C. C., Cowtan, K. D., Dodson, E. J., Emsley, P., Evans, P. R., Keegan, R. M., Krissinel, E. B., Leslie, A. G. W., McCoy, A., McNicholas, S. J., Murshudov, G. N., Pannu, N. S., Potterton, E. A., Powell, H. R., Read, R. J., Vagin, A., and Wilson, K. S. (2011) Overview of the CCP4 suite and current developments. *Acta Crystallogr. D67*, 235−242.

(34) McCoy, A. J., Grosse-Kunstleve, R. W., Adams, P. D., Winn, M. D., Storoni, L. C., and Read, R. J. (2007) Phaser crystallographic software. *J. Appl. Crystallogr. 40*, 658−674.

(35) Emsley, P., Lohkamp, B., Scott, W. G., and Cowtan, K. (2010) Features and development of Coot. *Acta Crystallogr. D66*, 486−501.

(36) Moriarty, N. W., Grosse-Kunstleve, R. W., and Adams, P. D. (2009) electronic Ligand Builder and Optimization Workbench (eLBOW): A tool for ligand coordinate and restraint generation. *Acta Crystallogr. D65*, 1074−1080.

DOI: 10.1021/acschemneuro.5b00038
ACS Chem. Neurosci. XXXX, XXX, XXX−XXX

(37) Hayward, S., and Lee, R. A. (2002) Improvements in the analysis of domain motions in proteins from conformational change: DynDom version 1.50. *J. Mol. Graphics Modell. 21*, 181−183.
(38) Hayward, S., and Berendsen, H. J. (1998) Systematic analysis of domain motions in proteins from conformational change: New results on citrate synthase and T 4 lysozyme. *Proteins: Struct., Funct., Genet. 30*, 144−154.

DOI: 10.1021/acschemneuro.5b00038
ACS Chem. Neurosci. XXXX, XXX, XXX−XXX